REPORT DOCUMENTATION PAGE	Form Approved OMB No. 0704-0188

1. REPORT DATE *(DD-MM-YYYY)*: 1 Aug 07

2. REPORT TYPE: Final Technical Report

3. DATES COVERED *(From - To)*: 1 Aug 2007-1 June 2009

4. TITLE AND SUBTITLE
Unique Advanced Comprehensive Laser-Doppler Velocimeter, Filtered Rayleigh Scattering and Laser-Induced Fluorescence System for Supersonic Turbulence Structural Measurement

5a. CONTRACT NUMBER

5b. GRANT NUMBER
FA9550-07-1-0556

5c. PROGRAM ELEMENT NUMBER

6. AUTHOR(S)
Gwibo Byun
Roger L. Simpson

5d. PROJECT NUMBER

5e. TASK NUMBER

5f. WORK UNIT NUMBER

7. PERFORMING ORGANIZATION NAME(S) AND ADDRESS(ES)
Aerospace and Ocean Engineering Department
Virginia Tech
Blacksburg, VA 24061

8. PERFORMING ORGANIZATION REPORT NUMBER

9. SPONSORING/MONITORING AGENCY NAME(S) AND ADDRESS(ES)
Air Force Office of Scientific Research
875 North Randolph Street
Arlington, VA 22203

10. SPONSOR/MONITOR'S ACRONYM(S)

11. SPONSOR/MONITOR'S REPORT NUMBER(S)
AFRL-AFOSR-VA-TR-2016-0693

12. DISTRIBUTION/AVAILABILITY STATEMENT
Distribution Statement A: Approve for public release. Distribution is unlimited

13. SUPPLEMENTARY NOTES

14. ABSTRACT
The proven laser-induced fluorescence (LIF) technique to measure the particle temperature, and the proven filtered Rayleigh scattering method to measure the gas density will be used simultaneously with the CompLDV for low uncertainty information on supersonic turbulent test flows. The accurate calculation of supersonic turbulent flow behavior for Air Force applications is still needed. It is clear from literature reviews that experimental research is needed on the structure of supersonic shock/boundary layer interaction (SBLI) over the rough wall surface using advanced experimental methods that can provide the needed turbulence structural information to develop computational models.

15. SUBJECT TERMS

16. SECURITY CLASSIFICATION OF:			17. LIMITATION OF ABSTRACT	18. NUMBER OF PAGES	19a. NAME OF RESPONSIBLE PERSON
a. REPORT	b. ABSTRACT	c. THIS PAGE			Gwibo Byun
	unclassified	unclassified			19b. TELEPHONE NUMBER *(Include area code)*

Final Report

DURIP AWARD A9550-07-0556

Unique Advanced Comprehensive Laser-Doppler Velocimeter, Filtered Rayleigh Scattering and Laser-Induced Fluorescence System for Supersonic Turbulence Structural Measurement

By

Gwibo Byun and Roger L. Simpson
Aerospace and Ocean Engineering Department
Virginia Tech
Blacksburg, VA 24061

June 1, 2009

This is the final performance report identifying the acquired equipment under the award (award No. A9550-07-0556). All equipment purchased will be used for the basic supersonic rough wall turbulent boundary layer research. This report also includes the primary calibration results of density and temperature using laser Rayleigh scattering and laser-induced fluorescence techniques, respectively. Finally, the future research project for which the equipment will be used is summarized.

1. The acquired equipment

The following equipment has been purchased in order to integrate and improve the unique LDV, FRS and LIF system for supersonic flow measurements as was described in the DURIP Proposal.

A. Verdi-V18 18W Nd:YOV4 diode-pumped laser
Supplier and price: Coherent, Inc., $125,000.00

B. 3 of ZT410PCI-21 digitizers
Supplier and price : ZTec Instrument, Inc., $19,485.00

C. 2 of UF3-4121 digitizers
Supplier and price : Strategic Test Co., $19,600.00

D. CS22G8 digitizer
Supplier and price : Gage Applied Technology, $11,145.30

E. 5 of Model 315 amplifier
Supplier and price : Sonoma Instrument Company, $12,070.00

F. 3 of LIF receiving unit
Supplier and price : Hamamatsu Co., $3,515.96

G. 2 of FRS receiving unit
Supplier and price : Hamamatsu Co., $1,602.28

H. 2 of high frequency Modulator and driver
Supplier and price : IntraAction Corp., $4,747.00

I. 2 of achromatic lens
Supplier and price : Ross Optical Industries, $822.00

J. High power fiber optics and laser-to-fiber coupler
Supplier and price : OZ Optics, $656.40

K. Optical filters and splitters for LIF and FRS receiving blocks
Supplier and price : Edmund Industrial Optics, $1,017.00

Sum of costs for items A ~ K = $199,660.94

2. Apparatus and data acquisition

In the section, the apparatus and data acquisition of density and temperature calibrations are presented. The calibration system is made of the items above and laser Rayleigh scattering (LRS) and laser-induced fluorescence (LIF) techniques are applied.

A. Variable pressure and temperature vessel

For density and temperature calibrations, the variable pressure and temperature vessel is designed as shown in Fig. 1. The pure pressurized air and pressure regulator are used to control the pressure inside and the flat glass plate is installed on the end to locate the measurement volume and detect scattered light. The heat tape and temperature controller are used to change the temperature inside. The pressure and temperature inside are recorded using the digital manometer and k-type thermocouple.

B. Optical setup and data acquisition

Figure 2 shows the schematic diagram of optical setup. The 532 nm CW laser light is focused by a 80 mm diameter and 250 mm focal length PCX and the resulting beam waist diameter is about 75 μm. The beam dump is mounted in the vessel in order to minimize the beam stray inside. The scattered light from the waist is detected by two identical achromatic lenses of 75 mm diameter and 300 mm focal length. These achromatic lenses minimize the aberration of various wavelength light scattered by fluorescence particles. The Rayleigh or fluorescence scattered light is transferred to the PMTs through a multimode fiber of 65 μm core diameter.

The black board is installed between the transmission and receiving optical parts in order to prevent the interference from the stray lights around the receiving achromats.

The Rayleigh scattered lights by air molecules have much lower intensity than ones by particles and the photon counting technique is applied for the density measurement. The PMT signal pulses due to the phones of Rayleigh scattering are counted in the specific record length. For the present measurement, two identical PMTs are used and two PMTs technique allows one to remove the shot noise contribution to the density fluctuation (Panda, 2007, Panda and Seasholtz, 2002). The shot noise of PMT is a random photo-electronic in nature and it is not correlated between two PMT signals. Therefore, the r.m.s. of density fluctuation is calculated using the cross-spectrum of these two PMT signals. The LRS receiving block is constituted by 50R50T beam splitter, 532 nm narrow bandpass filter and R7518P PMTs. The PMT outputs are recorded by 8bit CS22G8 digitizer and the photons above the threshold value are counted in Matlab.

On the other hand, the temperature measurement is performed by capturing the light intensity scattered by fluorescence particles, Rhodamine-B (Rh-B). This non-intrusive temperature measurement technique is proven well in many literatures and for the present calibration, the three-color bands are used for lower uncertainty and independence of optical path length as well (Lavieille et al., 2004, Maqua et al., 2006). The fluorescence particles are generated by the mixture of Rh-B, ethylenglycol and ethanol using Laskin nozzle. The fluorescent scattered lights are separated by 30T70R and 50T50R beam splitters for three PMTs. The interference optical filters, bandpass of 568 ± 5 nm, 600 ± 10 nm and long pass of 625 nm, are installed in front of each PMT. Figure 4 shows the three-color bands applied for the present measurement. The fluorescent light intensity is able to be measured by integrating each burst envelops of PMT signals. The low pass filters and triggering is used to get simultaneous three bursts. The 14bit ZT410PCI-21 digitizers are used to record and postprocess PMT outputs in LabView. Figure 4 shows the calibration apparatus and five receiving PMTs.

3. Calibration results

A. Density calibration

When the laser beam is passing through an air, the air molecules cause light scattering. The elastic light scattering by air molecules is called Rayleigh scattering. The light intensity of Rayleigh scattering is much lower than one of Mie scattering, which means that much less photons are captured by light detectors. Therefore, each photon generates PMT output like discrete pulse and the photon counting method counts these pulses of Rayleigh scattering in given time intervals, which depends on the density. Using the photon counting, the correlation between the number of photons collected during a specific time interval and the corresponding density is able to be measured.

The photon count rate ($N/\Delta t$) can be written as (Panda and Seasholtz, 2002)

$$\frac{N}{\Delta t} = \frac{\varepsilon P_0 n D \lambda \Omega}{hc} \frac{d\sigma}{d\Omega} \sin^2 \chi = Const \times n = Const' \times \rho \quad (1)$$

where, h = Planck's constant (6.63×10^{-34}J·s), c = speed of light (3×10^{9} m/s), ε = total light collection efficiency, P_0 = laser power (W), λ = laser wavelength (m), Ω = solid angle of receiving optics, $d\sigma / d\Omega$ = differential scattering cross-section (~ 10^{-32} m^2), χ = the angle between polarization direction of laser beam and the receiving vector, D = probe volume diameter (m) and n = number of density. Therefore, for a fixed optical setup, the photon count rate has a linear relation to the density. The average density, $\overline{\rho}$ can be written as

$$\overline{\rho} = a\left(\frac{N_{avg}}{\Delta t} + b\right) \quad (2)$$

where, a and b are the calibration constants and $N_{avg}/\Delta t$ is the average photon count rate during the record length. Ideally, the constant b should be zero from Eq.(1). However, 'b' in Eq.(2) denotes the effect of background noise due to the stray lights. Note that it is very important to minimize the light stray and it may be one reason that this Rayleigh scattering technique for density measurements has been applied mainly to jet flows.

It should be mentioned that the count rate is dependent on the PMT input voltage and the threshold value which one counts only the pulse higher than. Therefore, the optimum input voltage and the threshold value

need to be determined before the calibration. Increasing the input voltage and the threshold value, there is the flat region of count rates which is almost independent of them. The final PMT input voltage and the threshold value are determined the beginning of this flat region.

Figure 5 shows the calibration result of the count rate verse the density. The two PMT signals are sampled with 100 MHz rate during 5 sec. The incident laser power is 10 Watt. The mean count rate is averaged from 50,000 samples with the time interval Δt = 100 μs. It shows the linear relation as shown Eq.(2). The main error sources of average count rate and density is due to the shot noise and the resulting uncertainty is ±0.3 %.

B. Temperature calibration

The non-intrusive temperature measurement is able to be done using a temperature sensitive fluorescent tracer. This laser-induced fluorescence technique is widely used to measure the fluid temperature. The fluorescent light intensity (I_f) scattered by tracer particles which is dependent on the particle temperature can be written as (Lavieille et al., 2001)

$$I_f = K_{opt} K_{spec} V_c I_0 C e^{\beta / T} \qquad (3)$$

where, K_{opt} = optical constant, V_c = tracer particle volume (m^3), I_0 = incident laser intensity, C = molecule concentration of fluorescent tracer (mol/liter), T = absolute temperature and K_{spec} and β = constants depending only on the spectroscopic and physical properties of the fluorescent tracer. Therefore, the fluorescent light intensity is dependent on not only the temperature but also the particle size, incident laser intensity and tracer concentration. This undesired dependence can be removed using several color bands of fluorescent spectrum. The fluorescent light intensity in a spectral band [λ_{i1}, λ_{i2}] can be expressed by using a second-order expansion (Castanet et al., 2003).

$$
\begin{aligned}
I_f &= \int_{\lambda 1}^{\lambda 2} K_{opt}(\lambda) K_{spec}(\lambda) V_c I_0 C e^{\beta(\lambda)/T} d\lambda \\
&\approx K_{opti} K_{speci} V_c I_0 C e^{\frac{a_i}{T}+\frac{b_i}{T^2}}
\end{aligned} \tag{4}
$$

The subscript i denotes the spectral band i and the a_i and b_i are the coefficients of temperature sensitivity for the spectral band i. The ratio of fluorescent intensity between two spectral bands can be written as

$$
R_f = \frac{I_{f1}}{I_{f2}} = \frac{K_{opt1}}{K_{opt2}} \frac{K_{spec1}}{K_{spec2}} e^{\frac{a_1-a_2}{T}+\frac{b_1-b_2}{T^2}} \tag{5}
$$

This ratio in Eq.(5) is dependent only on the tracer temperature because the constants K_{opt} and K_{spec} are given for a fixed optical setup.

For the present measurement, the three-color spectral bands are selected as shown in Fig. 3. Figure 6 shows the three coincident bursts of PMT outputs generated by the fluorescent particles. The Rhodamine B (Rh-B) is used as the tracer and the mixture of Rh-B, ethylene glycol and ethanol is aerosolized by Laskin nozzles. The Rh-B concentration is about 6.7×10^{-4} mol/liter, which is lower than the critical concentration of self-quenching, 6×10^{-3} mol/liter (Lavieille et al., 2001). The incident laser power is 5 Watt and the sampling rate is 500 KS/s. Because of the lifetime of fluorescent light and re-absorption, the 2 kHz low pass filter is applied to get a smooth burst envelop. The mean ratio is averaged from more than 3,000 samples. Figure 7 shows the quadratic calibration curves between the intensity ratio and the temperature. The max variation of fluorescence ratio has about 38 %/K.

4. Brief description of supersonic rough wall flows research project

The proven laser-induced fluorescence (LIF) technique to measure the particle temperature, and the proven filtered Rayleigh scattering method to measure the gas density will be used simultaneously with the CompLDV for low uncertainty information on supersonic turbulent test flows. The accurate calculation of supersonic turbulent flow behavior for Air Force applications is still needed. It is clear from literature reviews

that experimental research is needed on the structure of supersonic shock/boundary layer interaction (SBLI) over the rough wall surface using advanced experimental methods that can provide the needed turbulence structural information to develop computational models. The instantaneous 3 components of velocity, the temperature, and the density are needed to determine all of the terms in the Reynolds-averaged continuity, momentum (RANS), energy, and turbulent Reynolds stress transport (RST) equations, assuming an equation of state to determine the instantaneous pressure. Data for non-equilibrium flows are severely needed. Little turbulence data for the supersonic rough wall flows exists because of the lack of previous experimental capability. All of these quantities will be measured in this AFOSR research.

A range of roughness of the roughness height, k and the ratio of roughness projected frontal area to flow to roughness area projected onto the mean surface, λ values will be used for both deterministic distributed roughness and more random roughness such as several grit sizes. Data for the test flow cases will be measured with variable height roughness surfaces. For some cases, uniformly distributed periodically spaced roughness elements up to 100micron high will be used as shown Fig. 8 for hemispheres. It is the super-hydrophobic surface produced by "Breath Figure" technique at the Virginia Tech. Such cases would allow researchers to determine actual effects of roughness geometry size, distribution and the flow structure around these elements. These size of roughness can be made of materials than can withstand supersonic speeds and temperatures. Other roughness shape surfaces of desired heights are prisms, pyramids, octagonal cones which can be manufactured on CNC milling machines from highly polished raw materials. The data for a given roughness shape should be obtained over a range of $0.01 < \lambda < 0.5$ and the effects of compressibility will be examined. The range of $k+ = (k\tau_{wall}/\rho)^{1/2}/\upsilon$ should cover both the transitionally rough($k+ < 50$) and fully rough($k+ > 50$) while keeping the $k/\delta < 0.025$.

Measurement will be made at M = 2.4 in low pressure gradient in the Virginia Tech Supersonic Blow-down Wind Tunnel over a range of $10{,}000 < Re_\theta < 25{,}000$ by adjusting the plenum pressure. Near adiabatic wall conditions can be produced on the rough surfaces by a polystyrene insulator and nearly constant wall temperature conditions can be produced by heated and cooled aluminum blocks that are thermally connected to a test surface.

Finally, the unique CompLDV, LIF and FRS system will be used to obtain the following quantities.

- All Reynolds-averaged and Favre-averaged quantities of mean velocities, temperature, density and pressure.
- Surface skin friction and heat flux from near-wall mean velocity and temperature profiles.
- Reynolds stresses, velocity fluctuation triple products.
- Dissipation rates and acceleration/velocity fluctuation correlations used to obtain velocity/pressure gradient fluctuation correlations.
- Temperature-velocity correlations for heat transfer structure.
- Velocity, temperature and density auto-spectra and cross-spectra.
- Spatial correlations and cross-spectra of velocity fluctuations using the second LDV system in order to provide data for the statistical coherency lengths of large-scale structures and the shock motion for comparisons with LES results.

The flow structure within the near-wall subsonic region will be examined and the relationship between the inner subsonic rough wall flow and the supersonic flow in the outer region will be described. These measurements will produce complete results for the Reynolds stress tensor in smooth and rough wall supersonic compressible flows. The data sets will be fully documented and available for use by others, especially those involved in LES studies in order to help the improvement of sub-grid scale modeling.

References

Castanet, G., Lavieille, P., Lebouché, M. and Lemoine, F., 2003, "Measurement of the temperature distribution within monodisperse combusting droplets in linear streams using two-color laser-induced fluorescence", Exp. Fluids, Vol. 35, pp.563-571.

Lavieille, P, Lemoine, F., Lavergne, G. and Lebouché, M., 2001, "Evaporating and combusting froplet temperature measurements using two-color laser-induced fluorescence", Exp. Fluids, Vol. 31, pp.45-55.

Lavieille, P., Delconte, A., Blondel, D., Lebouché, M. and Lemoine, F., 2004, "Non-intrusive temperature measurements using three-color laser-induced fluorescence", Exp. Fluids, Vol. 36, pp.706-716.

Maqua, C., Castanet, G., Lemoine, F., Doué, N. and Lavergne, G., 2006, "Temperature measurements of binary droplets using three-color laser induced fluorescence", Exp. Fluids, Vol. 40, pp.786-797.

Miles, R. B., Lempert, W. R. and Forkey, J.N., 2001, "Laser Rayleigh scattering", Meas. Sci. Technol., Vol. 12, pp.33-51.

Panda, J. and Seasholtz, R. G., 2002, "Experimental investigation of density fluctuations in high-speed jets and correlation with generated noise", J.Fluid Mech., Vol. 450, pp.97-130.

Panda, J., 2007, "Experimental investigation of turbulent density fluctuations and noise generation from heated jets", J.Fluid Mech., Vol. 591, pp.73-96.

Rawlett, A. M., Orlicki, J. A., Zander, N., Karikari,A. and Long, T., 2007, "Self assembled, ultra-hydrophobic micro/nano-textured surfaces", ARL-TN-275.

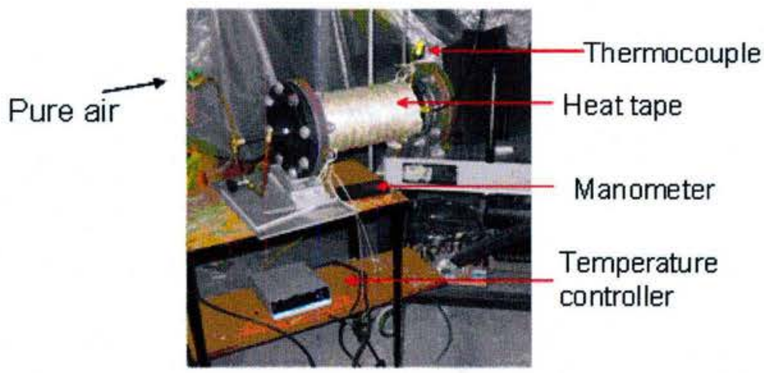

Fig. 1 Variable pressure and temperature vessel.

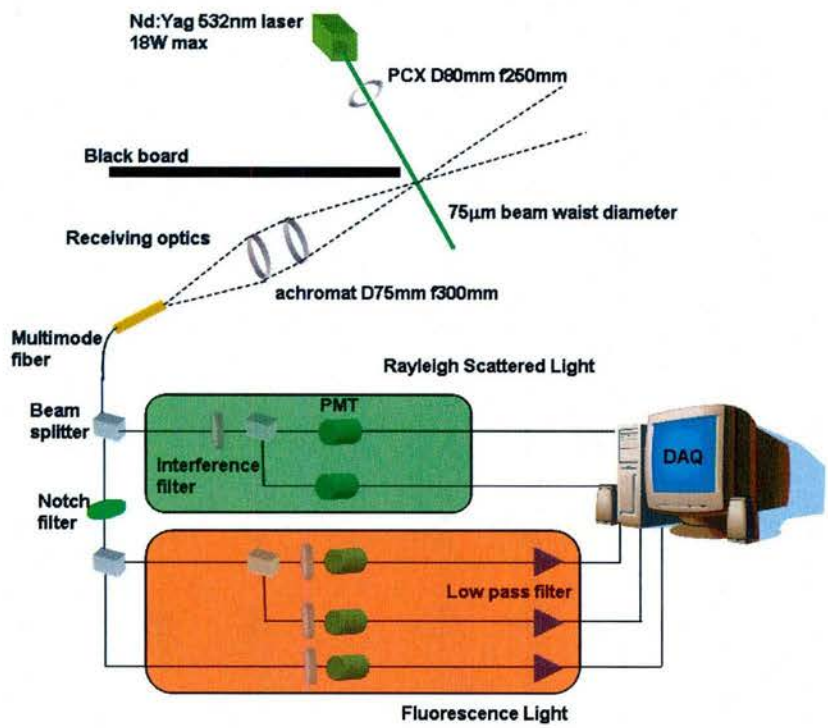

Fig. 2 Schematic diagram of optical setup.

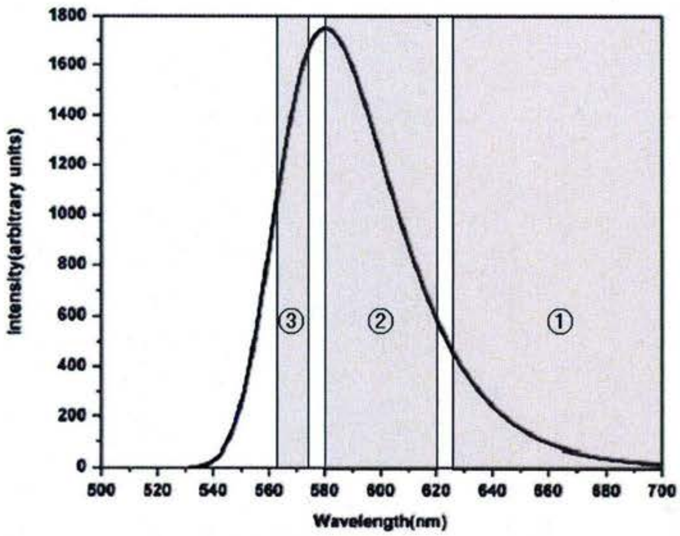

Fig. 3 Rh-B fluorescence spectra and
three-color bands for present LIF measurement; ①:625 nm↑, ②:600nm and ③:568 nm.

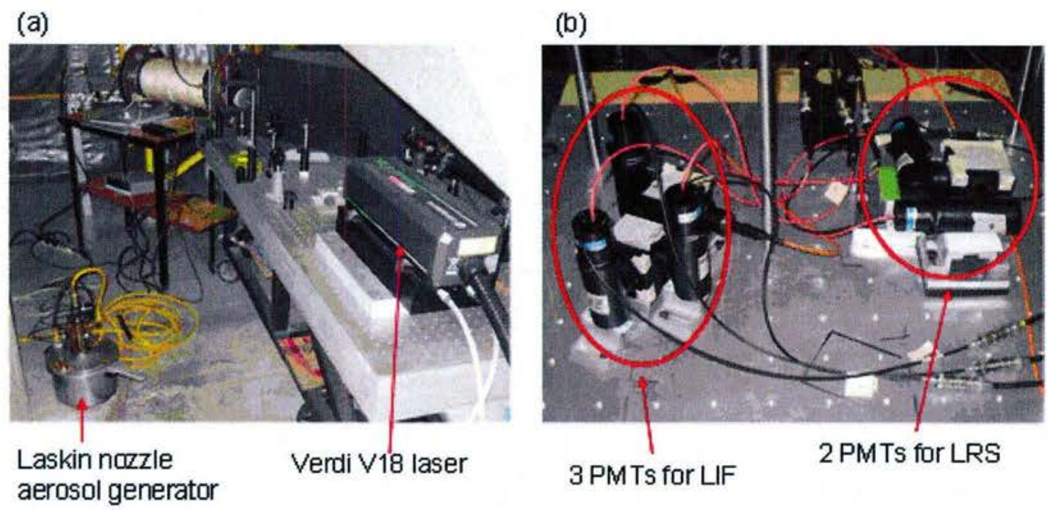

Fig. 4 Calibration apparatus(a) and receiving PMTs(b).

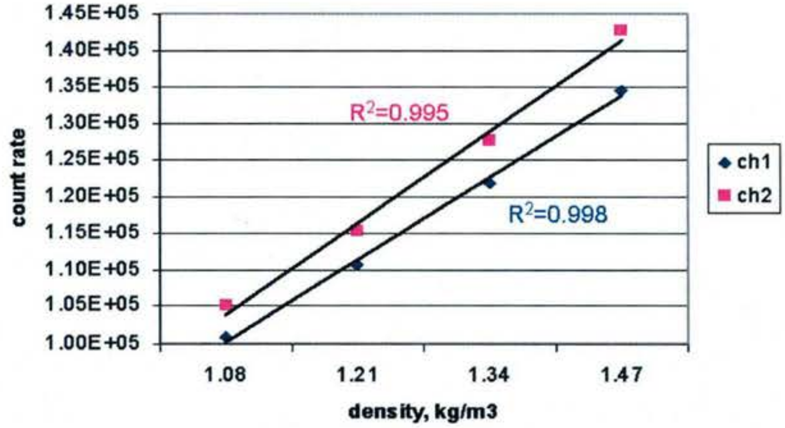

Fig. 5 The density calibration using laser Rayleigh scattering technique.

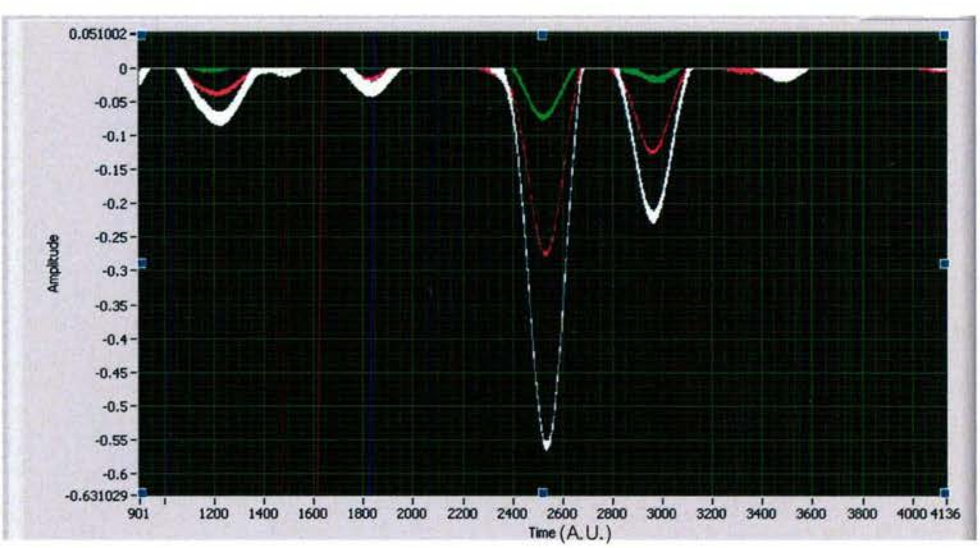

Fig. 6 Coincident three fluorescent bursts. White, 625 nm↑; red, 600 nm and green, 568 nm.

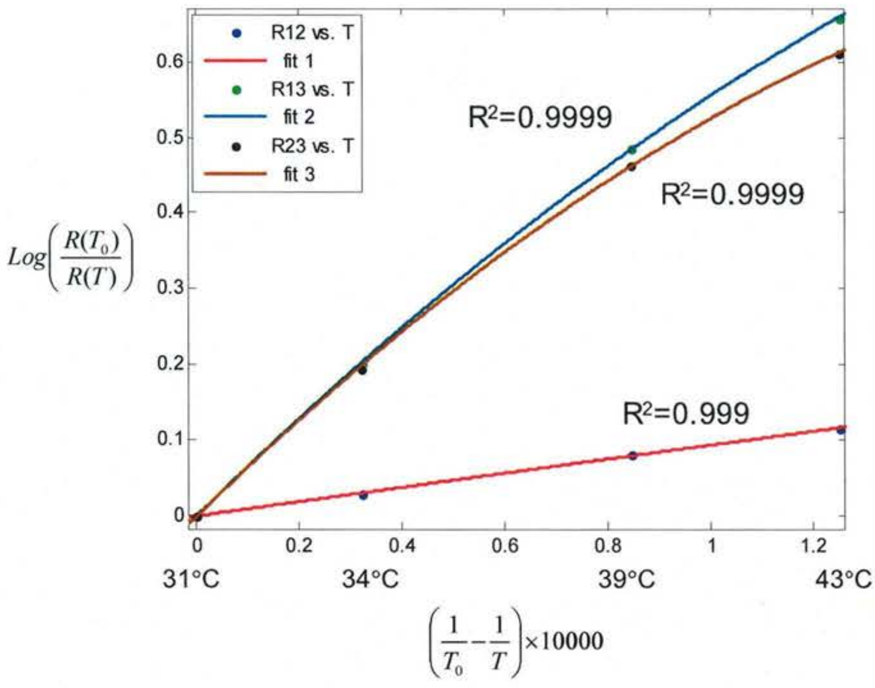

Fig. 7 The temperature calibration using laser-induced fluorescence technique. T_0 is the reference temperature. The intensity ratio R12, 625 nm↑ and 600 nm; R13, 625 nm↑ and 568 nm and R23, 600 nm and 568 nm.

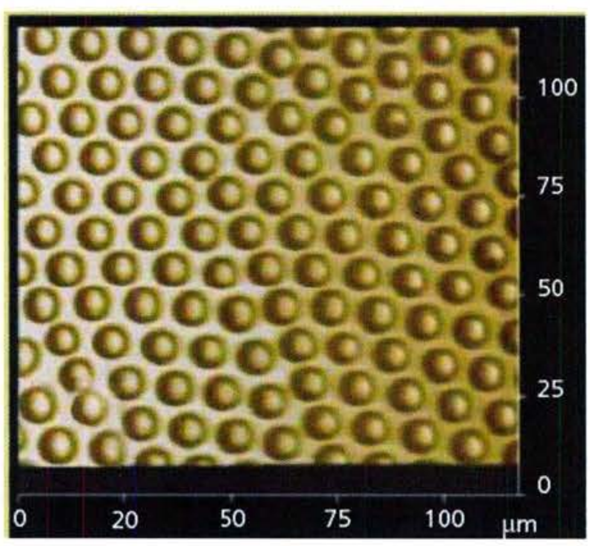

Fig. 8 Hemispherical pillars on a polystyrene template (Rawlett et al., 2007)